

University of Groningen

## Integral-Field Spectroscopy of SLACS Lenses

Czoske, Oliver; Barnabè, Matteo; Koopmans, L.V.E.

*Published in:*  
AIP Conference Proceedings

*DOI:*  
[10.1063/1.3141531](https://doi.org/10.1063/1.3141531)

**IMPORTANT NOTE: You are advised to consult the publisher's version (publisher's PDF) if you wish to cite from it. Please check the document version below.**

*Document Version*  
Final author's version (accepted by publisher, after peer review)

*Publication date:*  
2008

[Link to publication in University of Groningen/UMCG research database](#)

*Citation for published version (APA):*

Czoske, O., Barnabè, M., & Koopmans, L. V. E. (2008). Integral-Field Spectroscopy of SLACS Lenses. AIP Conference Proceedings, 1111, 137-140. DOI: 10.1063/1.3141531

**Copyright**

Other than for strictly personal use, it is not permitted to download or to forward/distribute the text or part of it without the consent of the author(s) and/or copyright holder(s), unless the work is under an open content license (like Creative Commons).

**Take-down policy**

If you believe that this document breaches copyright please contact us providing details, and we will remove access to the work immediately and investigate your claim.

*Downloaded from the University of Groningen/UMCG research database (Pure): <http://www.rug.nl/research/portal>. For technical reasons the number of authors shown on this cover page is limited to 10 maximum.*

# Integral-Field Spectroscopy of SLACS Lenses

Oliver Czoske, Matteo Barnabè and Léon V. E. Koopmans

*Kapteyn Astronomical Institute, P.O. Box 800, 9700 AV Groningen, The Netherlands*

**Abstract.** The combination of two-dimensional kinematics and gravitational lens modelling permits detailed reconstruction of the phase-space structure of early-type galaxies and sets constraints on the dark-matter distribution in their inner regions. We describe a project which combines integral-field spectroscopy from an ESO Large Programme using VIMOS on the VLT with deep HST ACS and NICMOS images to study a sample of 17 early-type lens galaxies at  $z \approx 0.1 - 0.3$ , drawn from the Sloan Lens ACS survey (SLACS).

**Keywords:** Early-type galaxies; dynamics; gravitational lensing

**PACS:** 98.52.Eh, 98.62.Dm, 98.62.Sb

## INTRODUCTION

Kinematic studies of early-type galaxies have a long history going back to the pioneering work of Rudolph Minkowski in the 1950s [1]. For a long time these studies were restricted to zero- (aperture integrated) or at best one-dimensional spatial resolution (using long slits). Over the last few years, new instruments with integral-field spectroscopic capabilities have become available on large telescopes that make it now possible to acquire two-dimensional kinematic fields across the visible face of local early-type galaxies. The largest systematic observations of this type to date have been performed using the SAURON instrument on the William Herschel telescope, resulting in kinematic maps and dynamical models of exquisite detail of a sample of 48 E and S0 galaxies [2, 3, 4]. An even larger follow-up project, ATLAS<sup>3D</sup>, has recently been started (see the contribution by P. Serra in this volume).

Spatially resolved observations of galaxy kinematics become much more difficult beyond the local universe, mainly due to the strong decrease in the number of resolution elements available to cover the galaxies. It is therefore useful to complement kinematic observations with other types of information, such as gravitational lensing, which becomes available for galaxies at redshifts  $z \gtrsim 0.04$ .

Like dynamics, lensing is sensitive to the total mass distribution (visible and dark). It does, however, not require the matter to be in dynamical equilibrium. Both dynamics and lensing individually show degeneracies, preventing some interesting physical parameters from being measured independently to good precision. A combined analysis can break the degeneracies and thus provide information about the galaxies that would not be available otherwise.

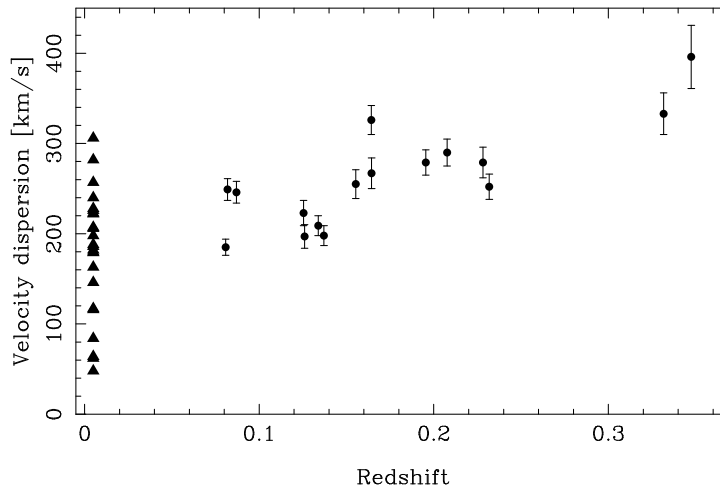


**FIGURE 1.** Distribution in redshift and velocity dispersion of the VIMOS-IFU (points with error bars, taken from [6]) and SAURON (triangles, taken from [3]) samples.

## SLOAN LENS ACS SURVEY (SLACS)

The Sloan Lens ACS Survey [5] has provided the largest sample of gravitational lens systems to date. The survey uses the SDSS luminous red galaxy sample and a quiescent subsample of the MAIN sample as its parent samples. A galaxy is considered a lens candidate if its SDSS spectrum shows emission lines at a higher redshift than its absorption-line redshift. Candidates are subsequently imaged with ACS or WFPC2 on HST to confirm the lens hypothesis and to provide the high-resolution imaging which forms the basis for the construction of detailed lens models. The full ACS sample currently comprises 89 confirmed lenses [6]; WFPC2 observations of further candidates are continuing.

Unlike many previous lens searches (e.g. the CLASS survey, [7]), SLACS is a *lens-selected* survey, i.e. the selection procedure guarantees the lenses to be bright and not outshone by the gravitationally lensed background sources. This makes SLACS a perfect sample for follow-up projects which combine the lensing information with other types of observation, such as the integral-field spectroscopy presented here.

## OBSERVATIONS

In an ESO Large Programme (177.B-0682), we have acquired integral-field spectroscopy of 17 lenses from the SLACS sample using the integral-field unit of VIMOS on the VLT UT3. Fig. 1 shows the distribution of our sample in redshift and velocity dispersion. Comparison to the SAURON sample shows that our sample is roughly equivalent to the high-mass half of the latter. However, our sample extends well beyond the local universe, covering redshifts from  $z = 0.08$  to 0.35 and thus permitting studies of the possible evolution of the structure of early-type galaxies over the last few Gyrs.

## COMBINED LENSING AND DYNAMICS ANALYSIS

The configuration of the gravitationally lensed source and the kinematic data (velocity and velocity dispersion) are modelled simultaneously in a fully self-consistent Bayesian framework. Full details on the analysis method and code are given by Barnabè and Koopmans [8].

Briefly, the algorithm starts from a parametric, axially symmetric model of the total gravitational potential,  $\Phi(R, z, \eta_k)$ , which in general depends on the parameters  $\eta_k$  in a non-linear way. For any given set of parameters, the lens reconstruction and the dynamical reconstruction can be formulated as linear models; the parameters to be reconstructed are the surface brightness distribution in the source plane and the phase-space distribution, respectively. The latter is built from two-integral components or “TICs” [9], which can be thought of as the collection of all orbits with a given energy  $E$  and angular momentum  $L_z$ . The non-linear parameters of the gravitational potential are then determined by maximising the Bayesian evidence, permitting objective comparison of different types of models.

The result of the analysis are thus the best values for the non-linear parameters  $\eta_k$  and reconstructions of the lensed background source and the phase space distribution function of the lens galaxy.

### FIRST EXAMPLE: SDSS J2321–097

As an example, we show in Fig. 2 the two-dimensional reconstructions of the gravitationally lensed source and the luminosity, velocity and velocity dispersion distributions in the system SDSS J2321–097 at redshift  $z = 0.082$  [10].

In most respects, SDSS J2321–097 is found to be a typical, massive elliptical galaxy. Its velocity dispersion,  $\sigma \approx 240 \text{ km s}^{-1}$ , would place it at the high-mass end of the SAURON sample, and like the most massive SAURON galaxies, SDSS J2321–097 is a pressure-supported slow rotator (as defined by [3]) with  $v/\sigma \approx 0.1$ .

In order to model the galaxy, a power-law mass density distribution  $\rho(r) \propto r^\gamma$  with axisymmetric ellipsoidal iso-density surfaces was assumed. The best-fitting logarithmic slope was found to be  $\gamma = -2.06^{+0.03}_{-0.06}$ , i.e. the density distribution is fully consistent with being isothermal. This confirms results from more simplistic analyses using the combination of lensing and kinematic data (e.g. [11]). Disentangling the contribution of dark and baryonic (i.e. mostly stellar) matter to the total density distribution requires further assumptions. In analogy to the maximum disk approach in modelling rotation curves of spiral galaxies we rescale the circularised stellar density profile (derived from the observed surface brightness) such that it maximises the contribution of the luminous component to the total density profile. This ‘maximum bulge’ approach provides a lower limit on contribution of the non-luminous components of about 30 per cent within the effective radius of the galaxy. This approach has been tested on simulated  $N$ -body systems (which do not obey any restrictive prescription of symmetry), showing that the correct dark matter fraction is recovered within  $\sim 10\%$  [12].

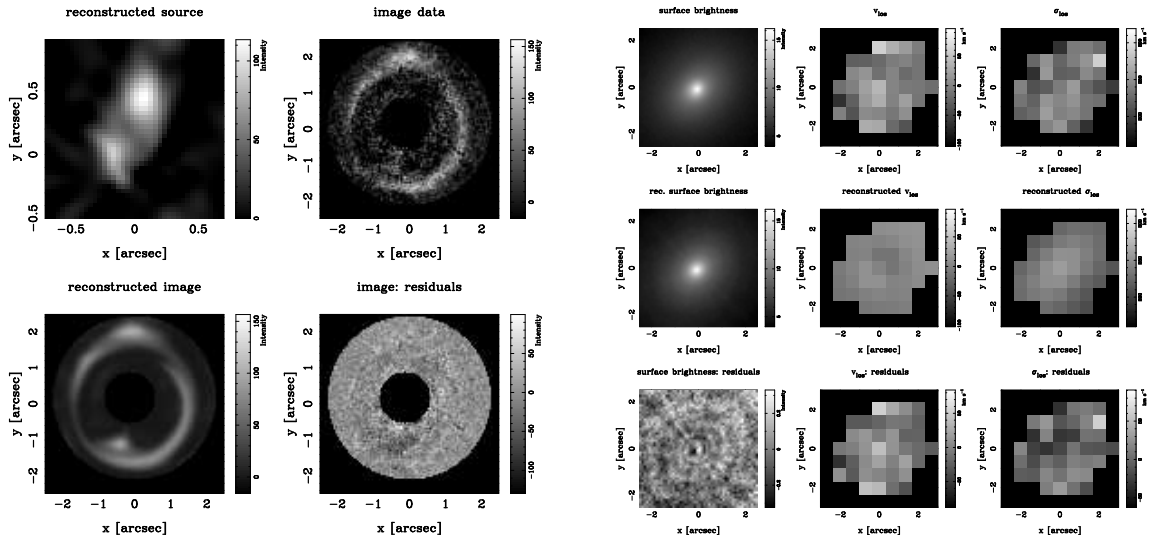


**FIGURE 2.** Lensing and dynamics reconstruction. The figures on the left show the observed gravitationally lensed source (after subtraction of the lens galaxy, top right), the reconstructed source in the source plane (top left) and in the lens plane (bottom left), as well as the residuals in the lens plane (bottom right). The figures on the right show the data in the top row: surface brightness of the lens galaxy, velocity  $v(x,y)$  and velocity dispersion  $\sigma(x,y)$ . The middle row shows the reconstructions from the phase space distribution function, and the bottom row the residuals.

## OUTLOOK

Apart from their use for reconstructing the mass structure of early-type galaxies, a stellar population analysis of the IFU spectra provides information on the age, metallicity and abundance ratios the stellar component (cf. [13]). Also, the stellar mass-to-light ratio can be estimated and used as further input towards the final goal of disentangling the baryonic and dark contributions to the total mass profile.

## REFERENCES

1. E. M. Burbidge, G. R. Burbidge, and R. A. Fish, *ApJ* **133**, 393 (1961)
2. E. Emsellem et al., *MNRAS* **352**, 721–743 (2004).
3. E. Emsellem et al., *MNRAS* **379**, 401–417 (2007).
4. M. Cappellari et al., *MNRAS* **379**, 418–444 (2007).
5. A. S. Bolton, S. Burles, L. V. E. Koopmans, T. Treu, and L. A. Moustakas, *ApJ* **638**, 703–724 (2006).
6. A. S. Bolton, S. Burles, L. V. E. Koopmans, T. Treu, R. Gavazzi, L. A. Moustakas, R. Wayth, and D. J. Schlegel, *ApJ* **682**, 964–984 (2008).
7. I. W. A. Browne et al., *MNRAS* **341**, 13–32 (2003).
8. M. Barnabè, and L. V. E. Koopmans, *ApJ* **666**, 726–746 (2007).
9. E. K. Verolme, and P. T. de Zeeuw, *MNRAS* **331**, 959–968 (2002).
10. O. Czoske, M. Barnabè, L. V. E. Koopmans, T. Treu, and A. S. Bolton, *MNRAS* **384**, 987–1002 (2008).
11. L. V. E. Koopmans, and T. Treu, *ApJ* **568**, L5–L8 (2002).
12. M. Barnabè, C. Nipoti, L. V. E. Koopmans, S. Vegetti, and L. Ciotti, *MNRAS* in press, arXiv:0808.3916 (2008).
13. S. C. Trager, S. M. Faber, and A. Dressler, *MNRAS* **386**, 715–747 (2008).